

## Effects of pump propagation and absorption on the gain distribution of longitudinally pumped Ni-like molybdenum x-ray lasers

Tsuneyuki Ozaki,<sup>1</sup> Hidetoshi Nakano,<sup>1</sup> and Hiroto Kuroda<sup>2</sup>

<sup>1</sup>*NTT Basic Research Laboratories, NTT Corporation, 3-1 Morinosato Wakamiya, Atsugi, Kanagawa 243-0198, Japan*

<sup>2</sup>*Institute for Solid State Physics, University of Tokyo, 5-1-5 Kashiwanoha, Kashiwa, Chiba 27-8581, Japan*

(Received 8 April 2002; revised manuscript received 22 July 2002; published 9 October 2002)

We reveal from simulations that in longitudinally pumped Ni-like Mo x-ray lasers, deformation of the temporal gain profile can occur, causing the x-ray laser pulse to have a steep rising edge. This is shown to be due to the rapid change in the inverse bremsstrahlung absorption when the main picosecond pulse pumps the cold preplasma.

DOI: 10.1103/PhysRevE.66.047402

PACS number(s): 52.59.Ye, 42.55.Vc

High repetition rate operation of x-ray lasers is an important factor for the active development of application experiments. There has been some energetic progress in this field using discharge-pumped argon scheme [1,2], and many more waiting to be brought to light. The authors have been focusing on longitudinally pumped transient-collisional-excitation (TCE) x-ray lasers as an answer to this challenging goal. By pumping preformed plasma from a longitudinal direction parallel to the x-ray laser beam, the pump energy that is required to saturate a Ni-like Mo x-ray laser is reduced to several hundred millijoules, making multihertz operation possible with present-day high-power laser technology. Li and Xu [3] have reported observations of large amplification with Ni-like Mo and Ne-like Ti ions using terawatt Ti:Sapphire laser system. A single 220-ps-duration prepulse was used to generate preplasma within a capillary, after which a 100-fs-duration short pulse was used to generate high gain. Ozaki *et al.* have shown that a Ni-like Mo x-ray laser with sub-milliradian divergence can be generated by irradiating a slab target with a 1060-nm-wavelength, 300-ps prepulse and a 475-fs main pulse [4]. The total energy in the two pulses was 150 mJ, which will make possible the multihertz operation. Combined with its high spatial coherence, this x-ray laser should attract numerous application experiments in various fields of science. In spite of these promising experimental results, the detailed physics of lasing in these experiments are not fully understood. However, the understanding of their mechanism is a must to make possible the optimization and efficient operation of this x-ray laser.

In this paper, we discuss the effects of pump pulse propagation on gain in longitudinally pumped Ni-like Mo x-ray lasers. We show that when the cold preplasma is irradiated by the high-intensity picosecond longitudinal beam, the inverse bremsstrahlung absorption rate decreases rapidly, due to the rapid change in the electron temperature of the preplasma. As a result, the incident picosecond pulse experiences a larger absorption at the front end of the pulse as compared with the trailing edge, causing the peak of the pump pulse to shift to later times. It is shown that the temporal gain profile is modified by this effect, and sufficiently large delay could even turn the gain negative.

The program used in this work consists of three codes, namely (i) a ray-trace code to model the propagation of the longitudinal beam through the preplasma, (ii) a hydrodynam-

ics code based on the hot-spot model [5] to calculate the change in the plasma parameters due to the interaction of the longitudinal pump with the preplasma, and (iii) an atomic kinetics code based on the collisional-radiative model [6] to calculate the population distribution among the various atomic levels. We use a differential equation in the paraxial form to calculate the propagation of rays in an optically inhomogeneous media [7]. In this work, we assume that preformed plasma with a quadratic density profile is produced prior to the irradiation of the main pump. Such a density profile works as a waveguide for the infrared longitudinal beam, and the index of refraction is calculated from the Drude model [8]. The code calculates the 18.9-nm  $4d-4p$  Ni-like Mo gain coefficient experienced by an x-ray beam traveling parallel to the waveguide axis. The spatial distribution of this gain is plotted for several x-ray beams that begin to propagate from the waveguide entrance at various times  $t_p$ . Here, an x-ray beam corresponding to  $t_p=0$  starts propagation when the peak of the main pulse arrives at the waveguide entrance.  $t_p$  is defined such that  $t_p<0$  corresponds to x-ray beams beginning propagation at the rising edge of the pump pulse, and  $t_p>0$  to those at the trailing edge. The relative timings of the x-ray beam, the main pump pulse, and the waveguide are schematically depicted in Fig. 1, for (a)  $t_p=0$ , (b)  $t_p<0$ , and (c)  $t_p>0$ .

Since the temporal gain duration of the x-ray laser in this work is of the order of several picoseconds, the difference in the propagation velocity between the longitudinal pump and the x-ray laser beam cannot be neglected. In the present work, we also take into account the difference in the propagation velocity of the infrared pump beam and the x-ray laser beam within the waveguide. One cause for such delay is the difference in the index of refraction and path length experienced by the two beams. However, both the x-ray laser beam and the infrared pump pulse are assumed to propagate parallel to the waveguide axis in this work. Therefore, the effects of difference in path length can be neglected. We denote the time delay due to the less-than-unity index of refraction of the pump beam as  $\Delta t_{ref}$ . Here  $\Delta t_{ref}\leq 0$ , that is, this effect causes the pump beam to propagate faster than the x-ray beam. We also include in this calculation the temporal deformation of the longitudinal pulse due to the rapid change in inverse bremsstrahlung absorption when the short longitudi-

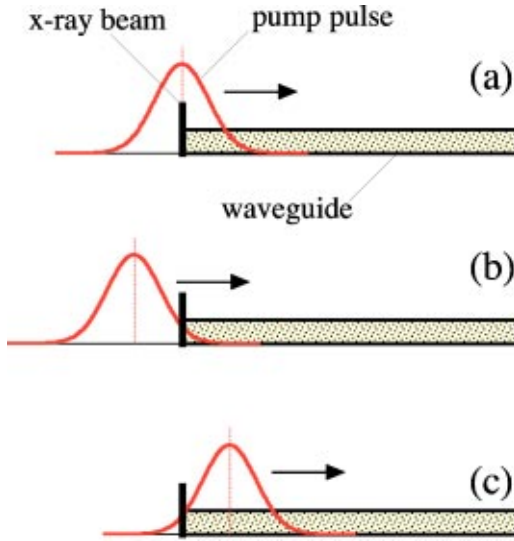


FIG. 1. Schematic diagram showing the relative timings of the pump pulse, x-ray beam, and the waveguide, for (a)  $t_p = 0$ , (b)  $t_p > 0$ , and (c)  $t_p < 0$ . The pump pulse enters the waveguide from the left.

nal pulse pumps the preplasma. The temperature of the preplasma rapidly increases from about 60 eV to greater than 1000 eV when a sufficiently intense longitudinal pump irradiates the preplasma. As a result, rapid decrease in inverse bremsstrahlung absorption occurs, and the incident picosecond pulse experiences a larger absorption at the front end of the pulse as compared with the trailing edge. This effect causes the peak of the pump pulse to shift to later times, resulting in an “apparent” delay. In this work, we simplify the calculation in order to conserve the CPU time consumed by the computer, by approximating this temporal deformation by a combination of “apparent” delay and intensity decrease of the pump peak.

The characteristics of this “apparent” delay due to absorption  $\Delta t_{abs}$  is investigated for a 1-ps-duration, 1- $\mu\text{m}$ -wavelength laser pulse propagating through preplasma. We assume an initial electron temperature of 65 eV for the preplasma, and the electron density is varied between  $2 \times 10^{20} \text{ cm}^{-3}$  and  $5 \times 10^{20} \text{ cm}^{-3}$ , which corresponds to typical initial conditions of the preplasma for Ni-like Mo x-ray laser. At pump intensities greater than  $10 \text{ PW/cm}^2$ , the rise in the electron temperature is rapid enough so that the change in inverse bremsstrahlung absorption during irradiation is relatively small, resulting in small  $\Delta t_{abs}$  values. A maximum in  $\Delta t_{abs}$  is observed between  $5 \times 10^{-3}$  and  $5 \times 10^{-2} \text{ PW/cm}^2$  for the electron densities investigated. For pump intensities below  $10^{-3} \text{ PW/cm}^2$ , the change in the electron temperature is not enough to cause the apparent delay. The total delay of the longitudinal pump beam can be calculated from  $\Delta t = \Delta t_{ref} + \Delta t_{abs}$ . For the case of Fig. 1(a) as an example, the x-ray beam will shift to the rising edge of the pump pulse after propagation for  $\Delta t > 0$ , and to the trailing edge for  $\Delta t < 0$ .

The atomic kinetics code includes Cu-like to Co-like ion levels, and thermal equilibrium is assumed for initial conditions. Opacity is included using escape factor formalism. In

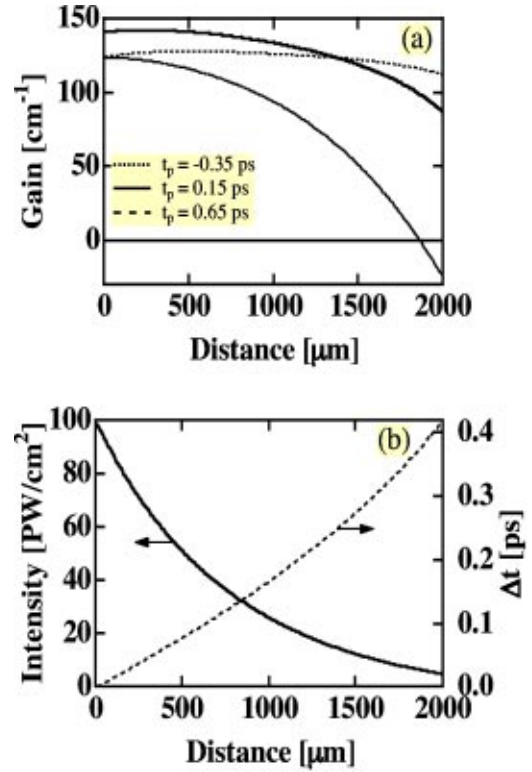


FIG. 2. (a) Distribution of the 18.9-nm gain and (b) intensity and delay  $\Delta t$  of the longitudinal pump along the plasma waveguide. The density and temperature of the preplasma at the waveguide center are  $3 \times 10^{20} \text{ cm}^{-3}$  and 65 eV, respectively. The origin of time  $t_p$  is at the peak of the 1-ps-duration longitudinal pulse.

the present work an optically thick condition is assumed, with a velocity gradient of  $10^5 \text{ cm/sec } \mu\text{m}$ . The 18.9-nm Ni-like Mo gain has been calculated using these codes and compared with the work of Nilsen [9], who used a much complex model. The results show that our compact code adequately reproduced results from the complex code, with the former typically resulting in conservative gain coefficients.

To keep the problem simple so that we can easily extract physics from the results, we assume in this work that the longitudinal pump beam propagates through a plasma waveguide maintaining a constant spot diameter  $w_o$ . Durfee *et al.* have shown [10] that such a condition can be realized if  $\Delta N_e = 1/\pi r_o w_o$ , where  $\Delta N_e$  is the difference between the electron density at the waveguide center ( $r=0$ ) and at  $r = w_o$ , and  $r_o$  is the classical electron radius. In such cases, the change in the pump intensity due to the focusing effect of the plasma waveguide can be neglected.

In Fig. 2(a), we plot the gain coefficient of the 18.9 nm Ni-like Mo x-ray laser as a function of the longitudinal distance along the plasma waveguide. The gain in this figure is that experienced by an 18.9-nm x-ray laser beam that starts to propagate parallel through the waveguide from 0  $\mu\text{m}$  (at the left of the figure) at times  $t_p = -0.35, +0.15$ , and  $+0.65 \text{ ps}$  from the peak of the longitudinal pump pulse. Here,  $t_p < 0$  and  $t_p > 0$  corresponds to the rising edge and trailing edge of the pump pulse, respectively, at the entrance of the waveguide. Conditions typical for saturated operation

of longitudinally pumped Ni-like Mo x-ray lasers are chosen in this work [6,11]. The electron density and temperature at the waveguide center is  $3 \times 10^{20} \text{ cm}^{-3}$  and 65 eV, respectively, and the longitudinal pump is 1053-nm-wavelength, 1-ps-duration pulse with peak intensity of  $100 \text{ PW/cm}^2$ . Under these conditions, a maximum gain coefficient of  $141 \text{ cm}^{-1}$  is obtained at the waveguide entrance at  $t_p = +0.15 \text{ ps}$ . The results show that the reduction in the gain coefficient after propagation through the 2-mm-long plasma is not critical, changing from  $141 \text{ cm}^{-1}$  at  $0 \text{ }\mu\text{m}$  to  $87 \text{ cm}^{-1}$  at  $2000 \text{ }\mu\text{m}$ . As a result, gain-length product of 25 is achieved at this time, which is enough to saturate the x-ray laser. This relatively large gain at the waveguide exit is due to the fact that the initial  $100 \text{ PW/cm}^2$  intensity of the longitudinal pump is much higher than that actually required for large gain.

The change in the peak intensity of the longitudinal pump and the delay time  $\Delta t$  of the infrared longitudinal beam relative to the x-ray laser beam is plotted in Fig. 2(b). The plasma absorbs more than 95% of the incident beam energy after propagating a distance of  $2000 \text{ }\mu\text{m}$  through the plasma. Yet the peak intensity of the longitudinal beam is still  $4.7 \text{ PW/cm}^2$ , which from conventional TCE x-ray laser measurements have been shown to be enough to generate large gain for the 18.9-nm Mo x-ray laser [12]. The energy that is required in the longitudinal pump to achieve a peak intensity of  $100 \text{ PW/cm}^2$  is 79 mJ for a  $10\text{-}\mu\text{m}$  spot diameter beam, which can be generated at multihertz repetition rates using present-day laser technology. This ability to achieve high intensities with relatively low pump energy is an advantage and one of the key points for the successful operation of the longitudinal pumping scheme.

An interesting phenomenon is seen to occur in Fig. 2(a). The gain coefficient at  $t_p = +0.65 \text{ ps}$  overtakes that at  $t_p = +0.15 \text{ ps}$  for distances greater than  $1400 \text{ }\mu\text{m}$  from the entrance of the plasma waveguide. One also notices that unlike the relatively gradual change in the gain coefficients with distance for  $t_p = +0.15$  and  $+0.65 \text{ ps}$ , the gain at  $t_p = -0.35 \text{ ps}$  shows a much rapid decrease, turning negative at the exit end of the waveguide. Upon inspection of the simulation outputs, we find that these phenomena are the results of the delay  $\Delta t$  between the x-ray laser beam and the longitudinal pump. Since the rays in this work are assumed to propagate parallel to the waveguide axis, the cause for change in  $\Delta t$  is the less-than-unity index of refraction and the apparent delay due to pump absorption. Since the refractive index of the plasma for the infrared longitudinal pump wavelength is smaller than that for the x-ray laser wavelength, the nonunity index-of-refraction forces the longitudinal beam to propagate faster and tends to reduce  $\Delta t$ . On the other hand, the apparent delay due to the change in inverse bremsstrahlung absorption increases  $\Delta t$ . Since Fig. 2(b) shows a monotonic increase in  $\Delta t$  with propagation through the waveguide, we see that the ‘‘apparent’’ delay effect is the dominant process in determining  $\Delta t$ .

Figure 3 is a schematic diagram showing the spatial distribution of the longitudinal pump laser intensity, x-ray laser gain, and the x-ray beam corresponding to  $t_p = 0$  at a given time and for (a)  $\Delta t = 0$  and (b)  $\Delta t > 0$ . The pump and x-ray

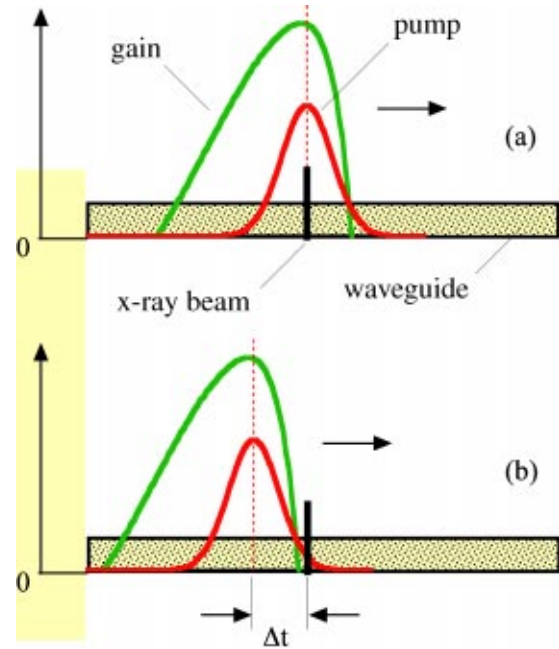


FIG. 3. Schematic diagram of the timing between the longitudinal pump, gain, and the x-ray laser beam at  $t_p = 0$ , for (a)  $\Delta t = 0$ , and (b)  $\Delta t > 0$ .

laser beams propagate from left to right, and so the right side of the pump beam corresponds to the rising edge. The abscissa corresponds to the spatial position within the waveguide, while the ordinate is the magnitude of either gain or longitudinal pump intensity in arbitrary units, and the zero-level is marked ‘‘0.’’ The unpumped 65-eV plasma has large negative gain at 18.9 nm, which turns positive before the peak of the pump laser. The gain rapidly increases at the rising edge of the pump, and reaches its maximum in about 1 ps, after which it monotonically decreases to zero in several picoseconds. The time at which the gain ceases is determined mostly by the opacity of the resonance lines and the pump intensity. Let us now focus at the gain observed by the x-ray laser beam at  $t_p = 0$ . The gain is near maximum for  $\Delta t = 0$ , as can be seen from Fig. 3(a). When  $\Delta t > 0$ , the longitudinal beam propagates slower than the x-ray laser beam, resulting in a delay of the pump. If the delay is too large, the x-ray laser beam will see a large reduction in gain occurring at the leading edge of the pump pulse. In the case of Fig. 3(b),  $\Delta t = +1 \text{ ps}$ , which results in a negative gain for an x-ray laser beam at  $t_p = 0$ . This effect is more pronounced at smaller  $t_p$ , and is the major cause for the  $t_p = -0.35 \text{ ps}$  gain to turn negative in Fig. 2(a). Conversely, this same effect will help to maintain or even increase the gain coefficient observed by an x-ray laser, if  $t_p$  is initially after the peak of the gain. This is because in this case a delay will cause the x-ray laser beam to experience a larger gain, if the pump intensity is the same.

Calculations show that  $\Delta t$  increases with an increase in the electron density of the plasma waveguide. Therefore, although a higher electron density results in a larger gain coefficient at the entrance of the waveguide, the apparent delay of the pump will limit the gain-length product attainable. To



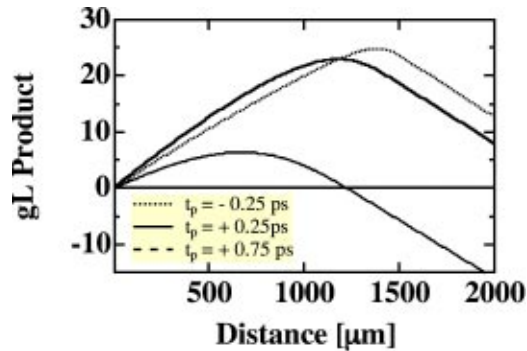


FIG. 4. Gain-length product of the 18.9-nm x-ray laser, for three times between  $t_p = -0.25$  ps and  $+0.75$  ps. The electron density and temperature at the center of the waveguide are  $5 \times 10^{20} \text{ cm}^{-3}$  and 65 eV, respectively.

show this tendency, calculations are performed for a waveguide with a relatively large central density of  $5 \times 10^{20} \text{ cm}^{-3}$ . Other parameters are kept equal to that used in Figs. 2(a) and 2(b). As is expected, a large gain coefficient of  $267 \text{ cm}^{-1}$  is observed at the waveguide entrance for  $t_p = -0.25$  ps from the peak of the pump, the time at which maximum gain is observed. The higher density of the waveguide causes a more rapid decrease in the pump intensity and a larger increase in  $\Delta t$  as the longitudinal beam propagates through the waveguide. As a result, the gain coefficient at  $t_p = -0.25$  ps turns negative at a distance of  $1190 \mu\text{m}$ . The longitudinal pump intensity at this point is  $3 \text{ PW/cm}^2$ , which is enough to generate a gain coefficient of  $200 \text{ cm}^{-1}$  for  $\Delta t = 0$  at this density. However,  $\Delta t$  at this same position is

$0.51$  ps, corresponding to one-half of the full width at half maximum duration of the longitudinal pulse.

The above unique temporal dependence of gain results in an interesting characteristic of this x-ray laser. In Fig. 4, we show the gain-length product as a function of distance from the waveguide entrance, for  $t_p = -0.25$ ,  $+0.25$ , and  $+0.75$  ps, and for a waveguide with central electron density of  $5 \times 10^{20} \text{ cm}^{-3}$ . The maximum gain-length product at  $t_p = +0.25$  ps is 23 (at  $1190 \mu\text{m}$  from the waveguide entrance), slightly smaller than that predicted for a  $3 \times 10^{20} \text{ cm}^{-3}$  density. The gain-length products at the same position are 0.76 and 23.1, for  $t_p = -0.25$  ps and 0.75 ps, respectively. That is, the 18.9-nm x-ray laser output intensity jumps from nearly zero gain to well over the saturation level within a time of 0.5 ps. These results show that when the longitudinal pump maintains a constant spot size through the waveguide, the temporal profile of the x-ray laser output will have a very steep sub-picosecond rise time, and a longer decay time at the trailing edge.

To summarize, we have shown that in a longitudinally pumped Ni-like Mo x-ray laser, an apparent delay of the longitudinal beam occurs, which is due to the rapid change in the inverse bremsstrahlung absorption when the main picosecond pulse pumps a cold preplasma. This phenomenon is found to greatly modify the gain observed by the x-ray laser beam. Simulations show that this delay in the longitudinal beam can accumulate with propagation through the gain medium, to a level large enough to change the gain coefficient to a negative value. As a result, this phenomenon is shown to be an important factor that must be taken into account when performing optimization calculation of longitudinally pumped transient-collisional-excitation x-ray lasers.

- 
- [1] I.A. Artiukov, B.R. Benware, J.J. Rocca, M. Forsythe, Yu.A. Uspenskii, and A.V. Vinogradov, *IEEE J. Sel. Top. Quantum Electron.* **5**, 1495 (1999).
- [2] B.R. Benware, M. Seminario, A.L. Lecher, J.J. Rocca, Yu.A. Uspenskii, A.V. Vinogradov, V.V. Ondratenko, Yu.P. Pershing, and B. Bach, *J. Opt. Soc. Am. B* **18**, 1041 (2001).
- [3] R. Li and Z.Z. Xu, *J. Phys. IV* **11**, 27 (2001).
- [4] T. Ozaki, H. Nakano, and H. Kuroda, *Technical Digest of CLEO/Pacific Rim 2001* (IEEE, Piscataway, 2001), p. 62.
- [5] K.G. Whitney and J. Davis, *J. Appl. Phys.* **45**, 5294 (1974).
- [6] R. Li, T. Ozaki, T. Kanai, and H. Kuroda, *Phys. Rev. E* **57**, 7093 (1998).
- [7] D. S. Goodman, in *Handbook of Optics*, edited by M. Bass, E. W. Van Stryland, D. R. Williams, and W. L. Wolfe, (McGraw-Hill, New York, 1995), p. 20.
- [8] H. Hora, *Plasmas at High Temperature and Density* (Springer-Verlag, Berlin, 1991).
- [9] J. Nilsen, *Phys. Rev. A* **55**, 3271 (1997).
- [10] C.G. Durfee, Jr., J. Lynch, and H.M. Milchberg, *Phys. Rev. E* **51**, 2368 (1995).
- [11] T. Ozaki, H. Nakano, and H. Kuroda, *J. Opt. Soc. Am. B* **19**, 1335 (2002).
- [12] Y. Li, J. Dunn, J. Nilsen, T.W. Barbee, Jr., A.L. Osterheld, and V.N. Shlyaptsev, *J. Opt. Soc. Am. B* **17**, 1098 (2000).